

QUASI –MONOENERGETIC NEUTRON BEAMS AT $E_n=30$ keV

Marita Mosconi¹, Ralf Plag¹, Michael Heil¹, Franz Käppeler¹, and Alberto Mengoni²

¹*Forschungszentrum Karlsruhe, Hermann von Helmholtz Platz 1, D-76344, Eggenstein-Leopoldshafen, Germany;*

²*International Atomic Energy Agency, Wagramer Strasse 5, A-1400 Vienna, Austria.*

Corresponding author: marita.mosconi@ik.fzk.de

The ${}^7\text{Li}(p,n){}^7\text{Be}$ reaction can be used for producing 30 keV neutron beams with a FWHM smaller than 10 keV. This neutron source can be employed to study inelastic scattering cross sections for low lying states down to excitation energies of 8 keV. With this approach, the ${}^{187}\text{Os}$ inelastic cross section for the first excited level at 9.75 keV has been measured at the 3.7 MV Van de Graaff of Forschungszentrum Karlsruhe using the Time-of-Flight technique. Depending on the energy of the proton beam, a resolution between 7 keV to 10 keV FWHM was achieved for the neutron beam. The actual measurement has been performed with a resolution of 9 keV FWHM. The stability of the experiment was controlled by monitoring the neutron beam with a FADC system. The low neutron yield from the ${}^7\text{Li}(p,n){}^7\text{Be}$ reaction at threshold has been compensated by the use of very efficient ${}^6\text{Li}$ -glass scintillators to detect the scattered neutrons. This measurement was part of a project for improving the Re/Os cosmochronometer.

I. INTRODUCTION

Inelastic scattering cross sections can be used to study the excitation of deformed nuclei^{1,2}. These data are also useful to evaluate the so-called stellar enhancement factor (SEF)^{3,4} used in nuclear astrophysics, which is required to take the effect of thermally populated nuclear states into account. For the latter aspect, measurements in the keV region are most important, where the necessary monoenergetic neutron beams are difficult to produce. This paper reports on the determination of the inelastic scattering cross section for the first excited level of ${}^{187}\text{Os}$ (9.75 keV above the ground state) at neutron energies of 30 keV. This result helps to constrain the neutron transmission functions for the excited levels and to calculate the radiative neutron capture cross sections for excited ${}^{187}\text{Os}$ nuclei using the Hauser-Feshbach statistical model⁵. The (n,γ) cross sections of the excited levels are required to evaluate the effective ${}^{187}\text{Os}$ averaged cross section³ at stellar temperatures around $kT=25$ keV, the typical thermal energy of the slow neutron capture (s)

process, which is responsible for the synthesis of ${}^{187}\text{Os}$ in Asymptotic Giant Branch (AGB) stars⁶.

An accurate value for the stellar cross section is mandatory for obtaining the s -process abundance of ${}^{187}\text{Os}$, which is important for the analysis of the galactic age via the ${}^{187}\text{Re}$ cosmochronometer^{7,8,9}. This clock is based on the 42.1 Gyr half-life of ${}^{187}\text{Re}$ and on the fact that the radiogenic abundance component of the daughter nucleus ${}^{187}\text{Os}$ can be based on s -process systematics¹⁰.

II. MEASUREMENT TECHNIQUES

The measurement of inelastic scattering cross sections for low lying excited states (level spacings of a few tens of keV) must rely on the direct detection of the inelastically scattered neutrons. However, the $(n,n'\gamma)$ technique¹¹ cannot be applied because the γ -transitions are too soft or highly converted. The most promising way for separating the inelastic and the elastic components is offered by the use of quasi-monoenergetic neutrons in combination with the Time-of-Flight (TOF) technique.

III. MONOENERGETIC NEUTRON BEAMS

Narrow neutron energy distributions in the keV region can be obtained with filtered beams using deep interference minima in the total cross section, e.g. at 24.4 keV in ${}^{56}\text{Fe}$ and at 45 keV in ${}^{52}\text{Cr}$ ⁽¹²⁾. Alternatively, quasi-monoenergetic beams can be produced in nuclear reactions. A prominent example is the ${}^7\text{Li}(p,n){}^7\text{Be}$ reaction, which can be used for producing monochromatic beams by adjusting the thickness of the ${}^7\text{Li}$ target to match the desired spectrum.

III.A. Monoenergetic Beams From The ${}^7\text{Li}(p,n){}^7\text{Be}$ Reaction

The ${}^7\text{Li}(p,n){}^7\text{Be}$ reaction represents a very prolific neutron source in the keV energy range. In nuclear astrophysics, it has been used extensively to measure the relevant neutron cross sections at stellar temperatures. It had been employed for TOF measurements by producing

continuous neutron spectra covering a wide energy range¹³ and also for activation measurements using the feature that a Maxwellian energy spectrum for $kT=25$ keV can be approximated with this reaction¹⁴. So far, low energy monoenergetic neutron beams have only been employed in some special cases, mostly in the context of the (n,n') cross section of ^{187}Os ^(15,16). The possibilities to produce monoenergetic beams of a few tens of keV are based on two characteristics of endothermic reactions:

1. the emission at threshold,
2. the angular dependence of the neutron energy.

The emission at threshold ($E_p=1.8811$ MeV) consists of neutrons with an energy of 30 keV emitted at zero degree. In a real experiment one is faced with a wider energy spectrum due to the energy distribution of the proton beam and due to straggling effects in the Li target.

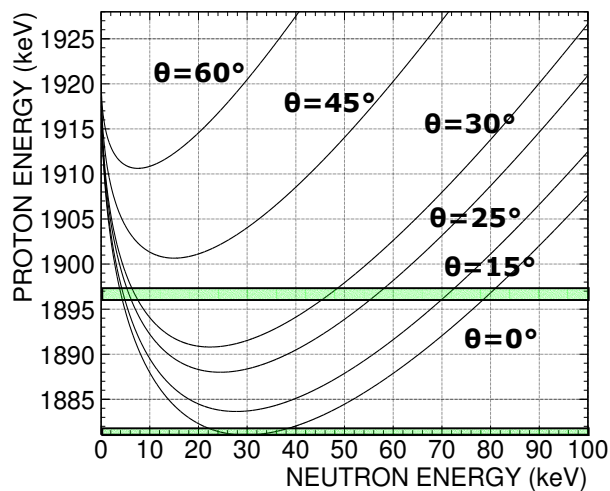


Fig. 1. The relation between neutron energy, proton energy, and angle of emission is shown according to the kinematics of the $^7\text{Li}(p,n)^7\text{Be}$ reaction^{17,18}. The shadowed areas would correspond to sharp neutron energy spectra. In a real experiment this would require very narrow proton energy distributions. At higher energies also very thin Li targets were necessary although the resolution can be improved by selecting particular angles.

At threshold, a Gaussian-like distribution centered at 30 keV^{18,15} can be produced. Up to now, this possibility has not been given much consideration because a narrow distribution is necessarily connected with a very small neutron yield. In case of the first excited level of ^{187}Os , the experimental neutron energy spectra were also too broad to resolve the inelastic component from low lying excited states¹⁵. The alternative for obtaining monoenergetic beams at those energies is by selecting a particular angle of emission. The kinematics of the $^7\text{Li}(p,n)^7\text{Be}$ reaction is sketched in Fig. 1. For example, a very narrow neutron energy distribution at 80 keV can be

obtained by the interaction of 1.897 MeV protons with a very thin ^7Li target and to restrict the angular acceptance of the experiment to a few degrees around the direction of the proton beam. The corresponding emission at 5 keV can be discriminated via TOF, for example. These two components are referred to as the first (higher energy) and second neutron group in the following.

III.A.1. Experimental Observations

The 3.7 MV Van de Graaff accelerator of Forschungszentrum Karlsruhe has been used to investigate the features of the $^7\text{Li}(p,n)^7\text{Be}$ reaction as a source of monoenergetic neutrons¹⁸. The proton beam was pulsed with a repetition rate of 1 MHz and a pulse width of 10 ns.

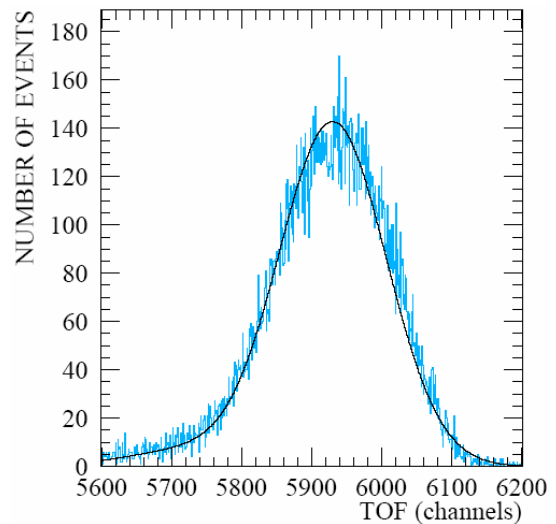


Fig. 2. TOF spectrum obtained using a metallic lithium target and a proton energy very close to the threshold of the $^7\text{Li}(p,n)^7\text{Be}$ reaction. The solid line is a fit of the experimental spectrum. The achieved FWHM is (7.7 ± 0.3) keV, corresponding to (5.6 ± 0.3) keV, if the time spread of the bunch is unfolded. Note that the lower energy part of the spectrum at the left exhibits a small tail.

In principle, the pulse width could be reduced to <1 ns by means of a Mobley buncher, but this was at the expense of an additional energy spread of the proton beam. It turned out that this led to unsatisfactory results so that the option of fast pulsing was discarded.

Because the goal was to measure the $^{187}\text{Os}(n,n')^{187}\text{Os}^*$ cross section close to the relevant astrophysical energies (8-25 keV), the emission at threshold was compared with solutions related to angle-selected spectra at higher proton energies presenting a suitable neutron energy. The TOF spectra were recorded

by a GS20 (NE908) ^6Li glass scintillator placed in front to the ^7Li target. Neutron spectra were taken by increasing the proton energy from threshold by several keV, yielding neutron spectra as illustrated by the two examples shown in Fig. 3. The two neutron groups appear already at proton energies 1 keV above threshold, thanks to a metallic Li target only 1 keV in thickness. At the lowest proton energy the first group is showing a pronounced tail that ends on the second. The fact that feature remains constantly as the proton energy is increased, indicates that this is not caused by moderation but is inherently due to the $^7\text{Li}(p,n)^7\text{Be}$ reaction itself.

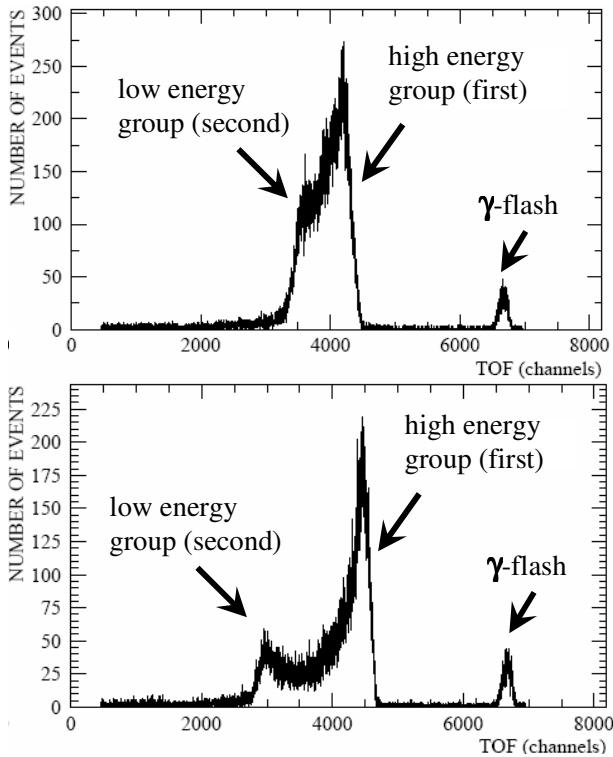


Fig. 3. Two TOF spectra taken at proton energies 2 and 4 keV above threshold using a thin Li target (1 keV in thickness). The detector was placed at 0 degree and at a flight path of 59.3 cm. The upper panel shows the first energy when the separation of the two neutron groups became visible ($E_p \sim 1$ keV above threshold). The separation is clearly improving at the higher proton energy (lower panel). The valley between the two groups can only be further reduced by decreasing the angular acceptance (i.e. by increasing the flight path).

A good spectrum obtained for the first group is presented in Fig. 4 with a zoom on the peak at $E_n = 53$ keV shown in the inset. Compared to the spectrum in Fig. 2, the peak exhibits a significantly larger tail towards lower energies. Obviously, in a scattering experiment this feature gives rise to a corresponding background, which would hamper

the reliable separation of the inelastic component. Therefore, the distribution centered at 30 keV, which is obtained at threshold, is to be preferred for the measurement of the inelastic scattering cross section to the first excited level of ^{187}Os .

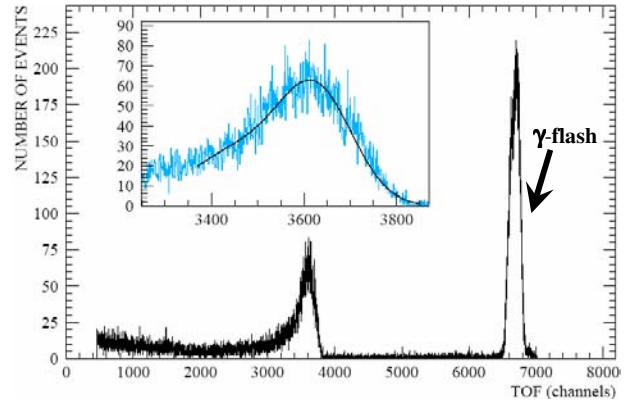


Fig. 4. TOF spectrum taken at $E_p \sim 6$ keV above threshold, using a LiF target ~ 1 keV in thickness and a flight path of at 89.5 cm. The higher γ -flash results from (p, γ) reactions on the fluorine. The center of the neutron energy distribution is (52.7 ± 0.1) keV. The FWHM is (8.2 ± 0.2) keV that becomes (6.4 ± 0.2) keV if the proton time distribution is unfolded.

IV. INELASTIC CROSS SECTION OF ^{187}Os

The inelastic scattering cross section to the first excited level of ^{187}Os was previously measured at 24.4 keV¹⁹, 34.4 keV²⁰, and 45 keV²¹ by using neutron filters and only once at 60.5 keV¹⁵ using a monoenergetic beam from the $^7\text{Li}(p,n)^7\text{Be}$ reaction. The achieved uncertainties (from 13% to 30%) were found to be too large to allow to perform reliable theoretical SEF calculations. Among these results, the measurement closest to the relevant stellar energy at 25 keV deviates strongly from a Hauser-Feshbach calculation of the (n,n') cross section supported all other data. This discrepancy and the rather large uncertainties of the published data motivated a new attempt for an accurate measurement using the 30 keV spectrum described before. In all measurements the shape of the elastic component was determined by means of reference sample, either by a natural lead sample (Refs. 19 and 21) or by an ^{188}Os sample prepared in the same way as that of ^{187}Os (Refs. 15 and 20). The sample material used in Refs. 15 and 20 (isotopically enriched metal powder from Oak Ridge National Laboratory) was available for the present measurement as well. The detection of a reference spectrum for purely elastic scattering is fundamental for the present TOF measurement, since the inelastic component can not be identified by the emission of a correlated γ -ray.

V. EXPERIMENTAL SETUP AT FZK

The accelerator was operated in pulsed mode with a repetition rate of 1 MHz. The target consisted of a metallic layer of natural lithium, which were evaporated onto silver backings to reduce the background from (p,γ) reactions. The experiment was performed at a special beam line where the object slit was located at the largest possible distance from the analyzing magnet. In this way, the energy stability of the proton beam could be optimized without losing beam intensity. In this way stable beam conditions could be maintained during the experimental runs, which lasted for several hours. Throughout the measurements, typical beam currents between 2 and 6 μA have been used.

A schematic sketch of the experimental setup is shown in Fig. 5. A GS20 (NE908) ⁶Li glass detector 3 mm in thickness and 3 cm in diameter served as a neutron monitor. It was located at a distance of 1.11 m from the target. Its output signal was connected with a Flash Analog to Digital Converter (FADC) to check the neutron energy distribution every two minutes to ensure energy stability. Depending on the status of the accelerator, the FWHM measured in the series of runs was between 7.6 and 9.5 keV.

At threshold, all neutrons are emitted into a narrow cone with an opening angle defined by the effective proton energy above threshold and by reaction kinematics (Fig. 1). From the maximum neutron energy it was calculated that the opening angle was always less than

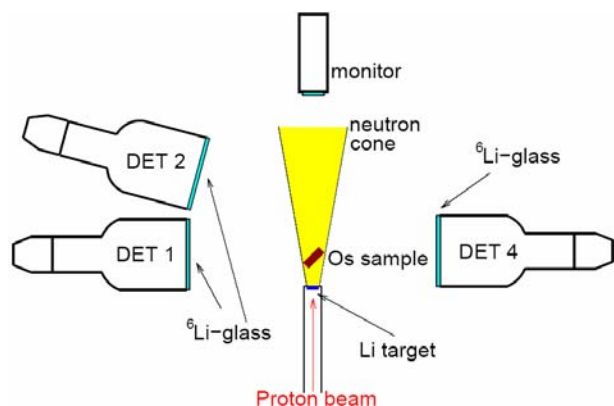


Fig. 5. Experimental setup (not to scale): The osmium samples were mounted at 4 cm from the ⁷Li target and were tilted at 45 degrees. The flight path to the detector is 26.1 cm. The neutron monitor is located at a flight path of 1.11 m.

30 degrees. Accordingly, the ⁶Li glass detectors for the scattered neutrons could be operated without any further shielding (Fig. 5). Only a small lead shield was placed around the neutron source in order to reduce the

γ-background in the detectors at 90 degrees (DET1 and DET4 in Fig. 5).

The ¹⁸⁷Os and ¹⁸⁸Os samples were encapsulated in thin aluminum cans 15 mm in diameter. The samples were glued onto a thin KAPTON[®] foil fixed to a carbon fiber frame, which was completely outside the neutron cone. The osmium samples were mounted at 4 cm from the ⁷Li target and were tilted at 45 degrees.

The ambient background was measured with a frame carrying an empty can. Scattered neutrons were detected by three KG2 (NE912) ⁶Li glass scintillators, two in symmetric positions at 90 degrees, and one at 120 degrees with respect to the proton beam. The flight path between the sample and these detectors was 26.1 cm. The signals from the 9823QKA Thorn EMI photomultipliers were analyzed by FADC with a resolution of 1 ns/channel. In this way the complete experimental information was stored for detailed off-line analyses, including a pulse shape discrimination between neutrons and γ-rays. This background reduction was achieved by restricting the accepted signals to the range around energy deposition of 4.8 MeV from the ⁶Li(n,α)T reaction. Although no perfect discrimination could be achieved, the γ-background could be reduced reasonably well.

Fig. 6 shows a typical TOF spectrum, with a pronounced peak due to the γ-flash produced by the

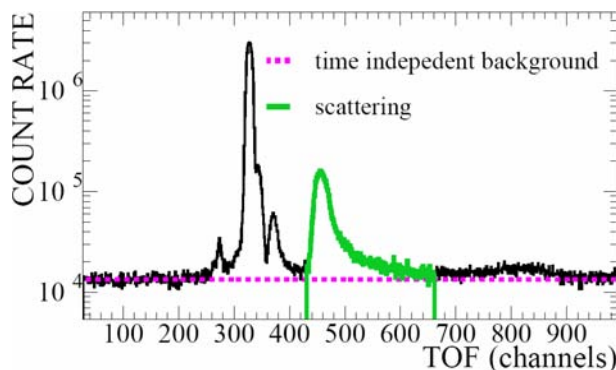


Fig. 6. Raw TOF spectrum taken with an ¹⁸⁷Os sample. In this case, the TOF runs from left to right. The structures starting from the left are due to γ-rays from proton interactions with the slits followed by the intense γ-flash due to proton interactions in the target. The smaller features at channels 340 and 380 on the shoulder of the flash and before onset of scattered neutrons at channel 450 are caused by (n,γ) reactions in the osmium sample and in the strong 5.9 keV resonance in the aluminium of the can. Apart from a small tail from these events the background is dominated by the time independent contribution. The bump around channel 800 is produced by neutron capture events in the monitor.

impact of the proton beam on the Li target. The largest background in the time window of the scattered neutrons (channels 450 to 660) was due to the ambient, time independent component. It required a correction of about 10%, which could be defined by the TOF region prior to the γ -flash as indicated in Fig. 6. The other background components could be corrected by the TOF spectra taken with the empty can.

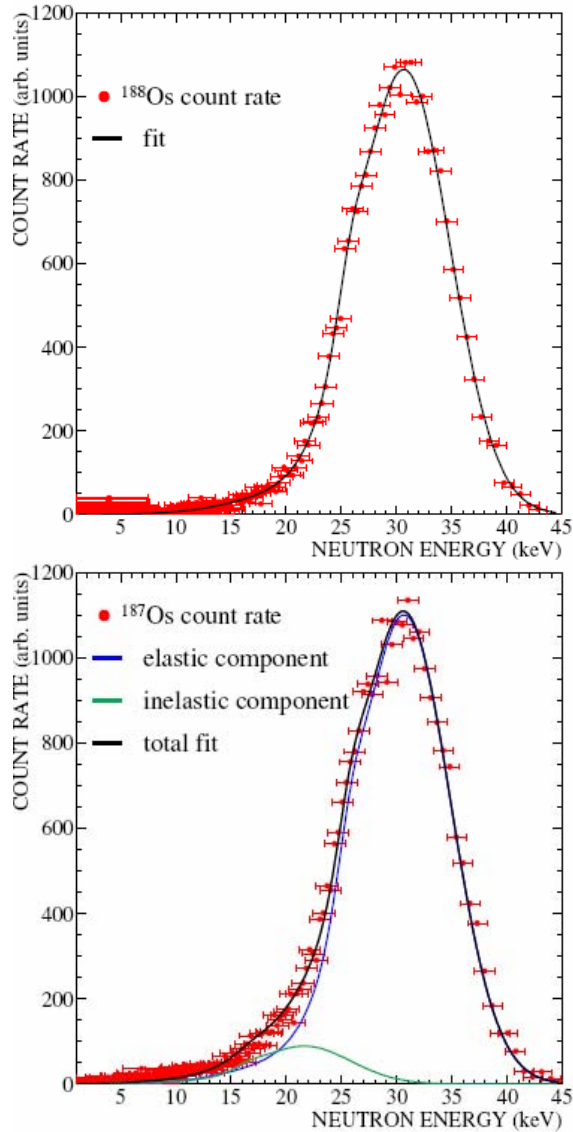


Fig. 7. Fits of the energy distribution measured with DET4 (see text). The fit of ^{188}Os was used to define the elastic distribution of ^{187}Os as well as the inelastic by shifting the shape by the energy of the first excited state at 9.75 keV. The only free parameters in the fit were the relative amplitudes of the two components in the ^{187}Os spectrum.

VI. ANALYSIS AND RESULTS

The neutron monitor allowed to sort the runs on the basis of the FWHM of the neutron distribution. Thus, it was possible to compare the count rates for ^{187}Os and ^{188}Os obtained under the same beam conditions. The best statistics was achieved with a FWHM of 9.5 keV. A first analysis was performed by comparison of the experimental spectra by using the fit of the elastic scattering in ^{188}Os for separating the inelastic component in ^{187}Os as shown in Fig. 7. To facilitate the fit, the TOF spectra were transformed into energy spectra, where the peaks could be described by the superposition of Gaussian functions.

Energywise, the inelastic distribution has the same shape as the elastic component, which is represented by the ^{188}Os spectrum, but shifted by the energy of the first excited level. This shift required a small correction for the neutron TOF between the Li target and the sample. The only free parameters in the fit were the relative amplitudes of the two components in the ^{187}Os spectrum.

While this way of analyzing the data neglects any sample effects, the comparison of the spectra taken with the three detectors indicated that they had to be considered at least in case of DET2. A bump interfering with the low energy tail of the scattering peak in the ^{187}Os TOF spectrum of this detector was creating an additional background. Therefore, a detailed GEANT-MICAP simulation of the experiment was carried out,

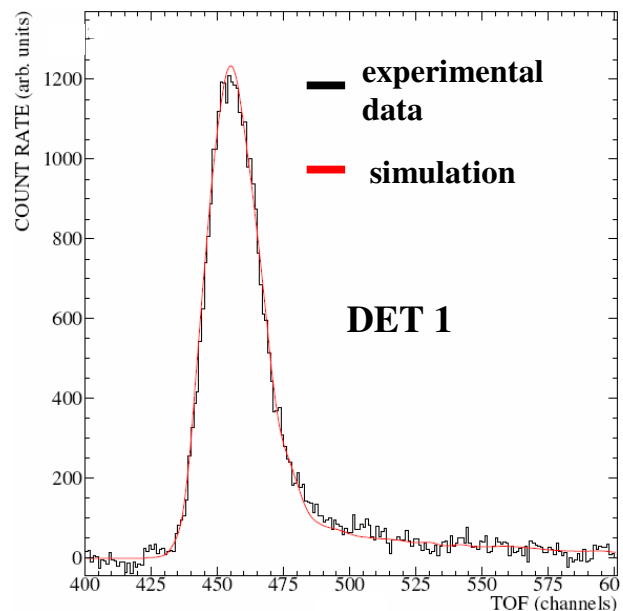


Fig. 8. Fit of the TOF spectrum taken with the ^{188}Os sample. All backgrounds beside the moderation effects are subtracted, thus illustrating the minor importance of moderation at 90 degrees.

which confirmed that this bump was due to a moderation effect caused by the different amounts of glue around the two samples. Since elastic scattering in hydrogen is strongly favouring the forward angles, only DET2 is affected by this phenomenon. The clear experimental signature of the moderation in the spectrum of DET2 could be used to obtain safe limits for the much smaller effects in DET1 and DET4.

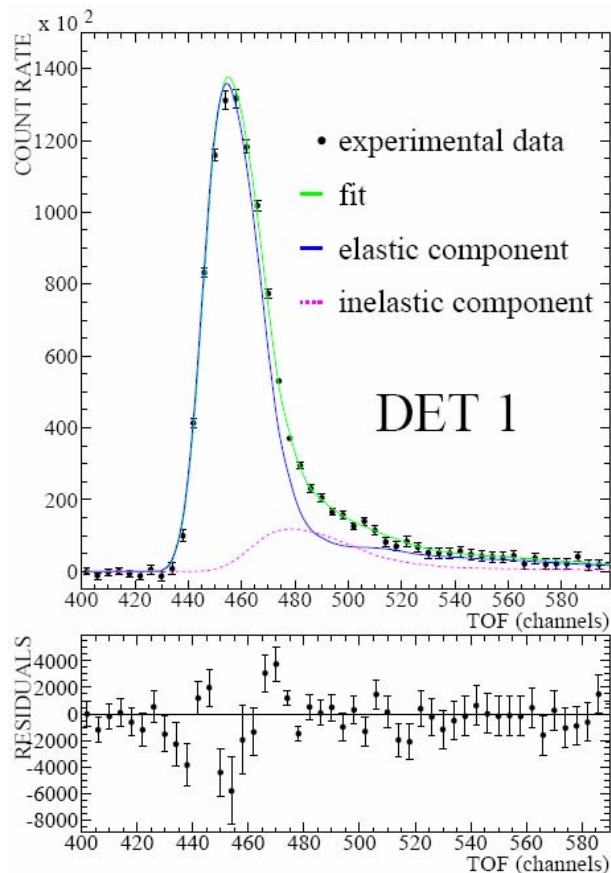


Fig. 9. Fit of the ^{187}Os TOF spectrum taken with DET1. The lower panel shows the residuals. The reduced χ^2 is 1.4. All backgrounds, including moderation, and scattering in the can and KAPTON[®] are subtracted. The error bars are dominated by systematic uncertainties related to background subtraction.

Since the simulations were performed by modelling the experimental setup in full detail including the proper neutron distribution generated by the $^7\text{Li}(p,n)^7\text{Be}$ reaction, it could be demonstrated that neutron scattering in the sample cans and in the KAPTON[®] foils contribute at most 10% to the elastic peak. The first step in analyzing the data by means of the simulations was to determine the parameters of the neutron distribution, i.e. by reproducing the elastic peak in the TOF spectrum of ^{188}Os as shown in Fig. 8. With this solution was then used to fit the elastic

component in the ^{187}Os spectrums and to characterize the inelastic component by the proper shift in energy.

The results are shown in Figs. 9 and 10. For DET2 the background from the moderation effects is dominating the TOF region of the inelastic peak. Therefore, the spectra of this detector have not been considered in further analysis. Although the inelastic contribution is much smaller, it is to be noted that it is impossible to fit the ^{187}Os spectrum using only the shape of the pure elastic component and that the inelastic component is always producing a clear signature.

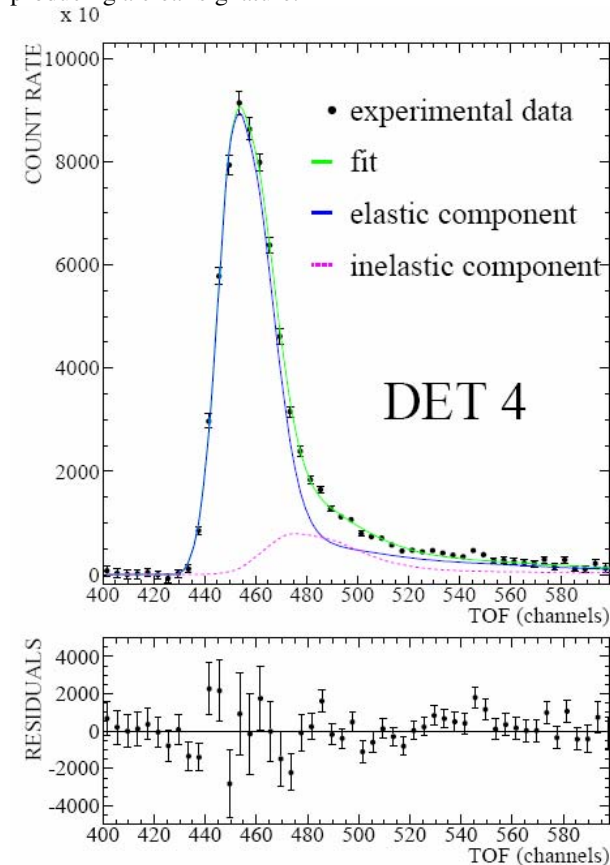


Fig. 10. Fit of the ^{187}Os TOF spectrum taken with DET4. The lower panel shows the residuals. The reduced χ^2 is 1.4. All backgrounds, including moderation, and scattering in the can and KAPTON[®] are subtracted. The error bars are dominated by systematic uncertainties related to background subtraction.

The results obtained by the different analyses illustrated in Fig. 7 and in Figs. 9 and 10 agree within 6%, thus underlining that sample effects are of minor importance for the detectors at 90 degrees.

The obtained cross section is shown in Fig. 11 together with the data from previous measurements. While good

agreement was found with the data from Refs 15, 20, and 21, the value for 24.4 keV reported in Ref. 19 can be ruled out, in particular because it is incompatible with the shape of the inelastic cross section obtained by the Hauser-Feshbach model.

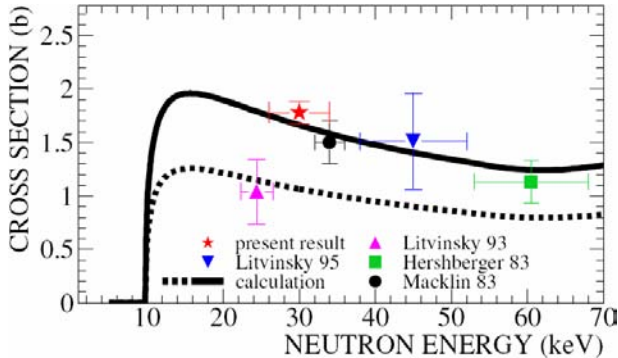


Fig. 11. Comparison of the present result (star) with previous data for the inelastic scattering cross section of ^{187}Os . The dotted line represents a calculation performed with the Hauser-Feshbach statistical model using the input from the total cross sections²² and the measured nuclear parameters from neutron resonance analyses²³. In the corresponding calculation shown by the solid line the inelastic scattering data are considered for improving the optical potential parameters used.

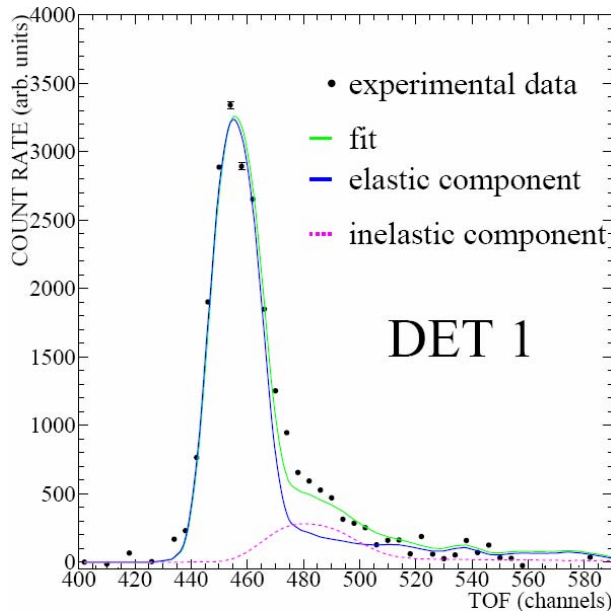


Fig. 12. Preliminary fit of a spectrum taken with a FWHM of 7.6 keV. The discrimination between the elastic and inelastic components is clearly improved, although a complete separation is not yet achieved.

VII. FURTHER IMPROVEMENTS

In the course of this experiment, neutron distributions with a sharper FWHM were detected with less statistics. This is illustrated in Fig. 12, which shows the TOF spectrum of ^{187}Os taken with a neutron energy distribution of 7.6 keV FWHM.

VIII. CONCLUSIONS

The inelastic scattering cross section to the first excited level of ^{187}Os was successfully measured with a neutron energy distribution of 9.5 keV FWHM. This measurement, combined with the accurate (n,γ) cross sections for $^{186,187,188}\text{Os}$ performed at the CERN n_TOF facility²⁴, allowed us to reduce the nuclear uncertainty related to the Re/Os clock from 13% to 3%²⁵. Distributions with a FWHM smaller than 8 keV could be observed, which are promising with respect to further improvements, provided that these spectra can be produced with sufficient intensity. A better energy stability of the proton beam would be an important step in this direction. Consequently, the measurement of inelastic cross sections for low lying excited levels below 8 keV appears to be possible using the neutron emission at the threshold of the $^7\text{Li}(p,n)^7\text{Be}$ reaction.

ACKNOWLEDGMENTS

We are grateful to D. Roller, E. P. Knaetsch, and W. Seith for providing continuous support at the 3.7 MV Van de Graaff accelerator

REFERENCES

1. D. F. COOPE, S. N. TRIPATHI, M.C. SCHELL, J. L. WEIL, and M. T. MAC ELLISTREM, "Strong Collective Excitations in Low Energy Neutron Scattering From Transitional Nuclei", *Phys. Rev. C*, **16**, 2223 (1977).
2. J. P. DELAROCHE, G. HAOUAT, J. LACHKAR, Y. PATIN, J. SIGAUD, and J. CHARDINE, "Deformations, Moments, and Radii of $^{182,183,184,186}\text{W}$ From Fast Neutron Scattering", *Phys. Rev. C*, **22**, 136 (1981).
3. Z. Y. BAO, H. BEER, F. KÄPPELER, F. VOSS, K. WISSHAK, and T. RAUSCHER, "Neutron Cross Sections for Nucleosynthesis Studies", *Atomic Data and Nucl. Data Tables*, **76**, 70 (2000).
4. A. MENGONI, "Neutron capture cross sections: from theory to experiment and back", *Nuclear Data for Science and Technology 2004*, Santa Fe, New Mexico (USA), 26 September- 1 October 2004, AIP conference proceedings, Vol. 769, p. 1209 (2005).

5. S. E. WOOSLEY and W. A. FOWLER, "A Nuclear Correction Factor For Re/Os Cosmochronology" *Ap. J.*, **233**, 411 (1979)
6. M. BUSSO, R. GALLINO and G. J. WASSERBURG, "Nucleosynthesis in Asymptotic Giant Branch Stars: Relevance for Galactic Enrichment and Solar System Formation" *Ann. Rev. Astron. Astrophys.*, **37**, 239 (1999).
7. D. D. CLAYTON, "Cosmoradiogenic Chronology of Nucleosynthesis", *Ap. J.*, **139**, 637 (1964).
8. K. TAKAHASHI, "Nucleo-cosmochronology and chemical evolution modellings", *Nucl. Phys. A*, **718**, 325 (2003).
9. M. ARNOULD and S. GORIELY, "Hope and inquietudes in nucleo-cosmochronometry", *Astrophysical Ages and Time Scales*, Hilo Hawaii (USA), 5-9 February 2001, ASP Conference Series, Vol. 245, p. 252, San Francisco (2001).
10. F. KÄPPELER, "The Origin of the Heavy Elements: the *s* Process", *Progr. Part. Nucl. Phys.*, **43**, 419(1999).
11. L. C. MIHAILESCU, L. OLÁH, C. BORCEA and A. J. M. PLOMPEN, "A New HPGe Setup at Gelina for Measurements of Gamma-ray production Cross Sections", *Nucl. Instr. Meth. A*, **531(3)**, 375(2004).
12. V. MAC LANE, C. L. DUNFORD and P. F. ROSE, *Neutron Cross Sections Vol 2*, pp. 168 and 184, Academic Press Inc., London (1988).
13. K. WISSHAK, F. VOSS, F. KÄPPELER, M. KRITČKA, S. RAMAN, A. MENGONI and R. GALLINO, "Stellar Neutron Capture Cross Section of the unstable *s*-process branching point ^{151}Sm ", *Phys. Rev. C*, **73**, 015802 (2006).
14. W. RATYNSKI and F. KÄPPELER, "Neutron Capture Cross Section of ^{197}Au : A Standard for Stellar Nucleosynthesis", *Phys. Rev. C*, **37**, 595 (1987).
15. R. L. HERSHBERGER, R. L. MACKLIN, M. BALAKRISHANAN, N. W. HILL and M. T. MACCELLISTREM, "Neutron scattering from Os isotopes at 60 keV and Re-Os nucleochronology", *Phys. Rev. C*, **28**, 2249 (1983).
16. M. T. ELLISTREM, R. R. WINTERS, R. L. HERSHBERGER, Z. CAO, R. L. MACKLIN and N. W. HILL, "Neutron Scattering in ^{189}Os for Nucleosynthesis rates of the odd-A isotopes and nucleochronology", *Phys. Rev. C*, **40(2)**, 519 (1989).
17. J. MONAHAN, "Kinematics of neutron producing reactions", in J. B. Marion and J. L. Fowler, *Fast Neutron Physics, part I*, pp. 49-72, Interscience Publisher Inc., New York (1960).
18. M. MOSCONI, "Re/Os cosmochronometer: neutron scattering in ^{187}Os at stellar energies", *Master Thesis*, Università degli Studi di Torino (2002).
19. L. L. LITVIKSKY, "Neutron Cross Sections of ^{187}Os and Their Analysis With a Possible Correlation of the Elastic and Inelastic Scattering Channels", *Phys. Atom. Nucl. (trad. Yad. Fiz.)*, **56(1)**, 17(1993).
20. R. L. MACKLIN, R. R. WINTERS, N. W. HILL and J. A. HARVEY, " $^{187}\text{Os}(n,n')$ Inelastic Cross Section at 34 keV", *Ap. J.*, **274**, 408 (1983).
21. L. L. LITVIKSKY, Y. A. ZHIGALOV, V. A. LIBMAN, A. V. MURZIN, A. M. SHKARUPA, "Inelastic Scattering of 45 keV Neutrons by ^{187}Os ", **58(2)**, *Phys. Atom. Nucl. (trad. Yad. Fiz.)*, 164 (1995).
22. National Nuclear Data Center, <http://www.nndc.bnl.gov/>.
23. S. F. MUGHABGHAB, *Atlas of neutron resonances*, pp.76-(1-7), Elsevier, New York (2006).
24. M. MOSCONI and THE n_TOF COLLABOATION, "Experimental challenges for the Re/Os clock", *Nuclei in the Cosmos IX*, 25-30 June 2006, Geneva (Switzerland), Proceedings of Science, PoS(NIC IX)055 (2006).
25. M. MOSCONI, M. HEIL, F. KÄPPELER, A. MENGONI, and R. PLAG, "Inelastic neutron scattering cross section of ^{187}Os at 30 keV", *Nuclear Data for Science and Technology 2007*, Nice (France), 23-27 April 2007, *in press* (2007).